

¹⁴We have also performed calculations which include the unlinked part of the biexcited clusters $\frac{1}{2}\hat{T}_1^2$. These calculations prove the complete negligibility of these terms, since their inclusion does not change the results obtained with the *C* approximation (up to eight decimal places, at least). Clearly, the cubic terms $(1/3!)\hat{T}_1^3$ will give an even smaller effect and may be safely disregarded. This result is also indicated by considering the lowest order of perturbation theory in which these terms will appear.

¹⁵The number of linearly independent singlets, and of corresponding \hat{t}_3 matrix elements, may be smaller than this maximum in some cases because of spatial symmetry requirements. In any event it can be shown that there always is one more \hat{t}_3 matrix element than the corresponding number of linearly independent CI singlets.

¹⁶The atomic orbital integrals were recomputed (to an

accuracy of better than 10^{-6} a.u.) using R. M. Stevens' program [Program 161, Quantum Chemistry Program Exchange, Indiana University, 1970 (unpublished)]. Errors of up to 0.7×10^{-4} a.u. were found in the original integrals used in Ref. 5. The CI results were recomputed using programs written by A. Pipano (unpublished).

¹⁷Actually the smallness of unlinked triexcited clusters is understandable in terms of the smallness of \hat{T}_1 , i.e., "the effect of correlation on orbitals", Ref. 7(b).

¹⁸Z. Gershgorin and I. Shavitt, Intern. J. Quantum Chem. 2, 751 (1968).

¹⁹When exploiting the space symmetry, the number of \hat{t}_1 and \hat{t}_2 matrix elements and, correspondingly, of Eqs. (A1) is reduced by the same number as the order of CI including monoexcited and biexcited states.

Electron Binding Energies, X-Ray Spectra, and *L*-Shell Fluorescence Yields in Curium ($Z = 96$)

Y. Y. Chu* and M. L. Perlman*

Chemistry Department, Brookhaven National Laboratory, Upton, New York 11973

and

P. F. Dittner† and C. E. Bemis, Jr.†

Transuranium Research Laboratory, Oak Ridge National Laboratory, Oak Ridge, Tennessee 37830

(Received 8 June 1971)

The Cm *K* x-ray spectrum from the decay of ²⁴⁹Cf and the Cm *L* x-ray, internal conversion, and γ -ray spectra associated with the 42.9-keV *E2* transition in the α decay of ²⁵⁰Cf were measured at high resolution. From these data accurate values for the binding energies of *K*, *L*₁, *L*₂, *L*₃, *M*₁, *M*₂, *M*₃, *M*₄, *M*₅, *N*₁, *N*₂, *N*₃, *N*₄, *N*₅, *O*₂, *O*₃, *O*₄, and *P*₃ electrons in Cm were obtained. Values were derived also for the *L*-subshell fluorescence yields in Cm: $\omega_1 = 0.28 \pm 0.06$, $\omega_2 = 0.55 \pm 0.02$, and $\omega_3 = 0.63 \pm 0.02$.

INTRODUCTION

The experimental determination of accurate values for the energies of atomic electron levels provides information with which theoretical calculations of atomic structure may be compared, and, as a practical matter, these values make available energy reference standards for β - and γ -ray spectroscopy. Further, the x-ray spectra of trans-fermium elements could provide a means for their identification, and Carlson, Nestor, Malik, and Tucker¹ were thus prompted to calculate electron binding energies for *Z* values from 96 to 120. They used relativistic Hartree-Fock-Slater finite-nuclear-size wave functions and made small corrections to these results by extrapolating experiment-calculation energy differences known at lower *Z* values. It is of interest to compare these binding energies as far as possible with measured values. For $Z > 95$ experimental electron-binding-energy

information is limited; *K* through *M*₃, *N*₁, and *O*₁ measurements have been made in berkelium² ($Z = 97$); and recently measurements for *K* through *M*₃, *N*₁, *N*₂, *N*₃, and *O*_{2,3} have been published³ for californium ($Z = 98$). Experimental information on binding-energy differences is available for elements of $96 \leq Z \leq 100$ from very accurate measurements of *K* x-ray spectra.⁴ There are presented in this paper measurements made on radiations of ²⁴⁶Cm and ²⁴⁵Cm from which electron binding energies and *L*-subshell fluorescence yields in curium ($Z = 96$) have been derived.

EXPERIMENTAL METHODS

About 17% of the α decay of 13-yr ²⁵⁰Cf produces the 42.9-keV first-excited state of ²⁴⁶Cm, which decays by a highly converted pure *E2* transition.⁵ Measurements of the energies of the internal-conversion-electron lines and the unconverted γ ray

were combined to obtain some of the L -, M -, N -, O -, and P -electron binding-energy values. By combination of these binding energies with energies of the Cm L x rays, also observed with ^{250}Cf sources, a number of other electron-level energy values were derived. K -electron binding energies were determined by combination of L - and M -electron binding energies with the energies of Cm K x rays measured with a ^{249}Cf source ($t_{1/2} = 360$ yr). Fluorescence yields for the L subshells were obtained from measurements with ^{250}Cf . Here all primary L vacancies are produced by internal conversion of the 42.9-keV γ ray; and the fluorescence yield results could be calculated from the intensity of the unconverted gamma ray, the intensities of the L x-ray lines, the L -subshell internal conversion coefficients,⁶ and available information on the relevant Coster-Kronig probabilities.

Sources

The nearly isotopically pure (>99%) sources of ^{250}Cf used for much of the L x-ray spectroscopy were prepared by separation of daughter from the decay of 3.2-h ^{250}Bk , itself the product of neutron capture in ^{249}Bk . Rare-earth fission-product activities were removed from the initially separated Cf by repeated chemical purifications. Sources of 360-yr ^{249}Cf used for the K x-ray spectroscopy were prepared in a similar way from a 2-month accumulation of Cf daughter resulting from the decay of isotopically pure 314-day ^{249}Bk . Internal conversion is responsible for the Cm K x-ray emission in ^{249}Cf decay. Some L x-ray measurements and all of the internal-conversion-electron spectroscopy were done with a source of ^{250}Cf prepared isotopically pure in the electromagnetic separator at the Los Alamos Scientific Laboratory by collection of 55-keV ions on 0.001-in.-thick aluminum foil.⁷ Autoradiography showed the deposit to be in the form of a rectangle about 1 mm wide and 12 mm long.

Electron Spectrometry

Conversion-electron spectra were measured with an automatically operated 50-cm-radius $\pi\sqrt{2}$ iron β -ray spectrometer.^{8,9} A proportional counter, through which butene gas at a pressure of 19 Torr was slowly pumped, was employed as the detector. For the range of electron energies in these experiments, corrections for absorption in the 54- $\mu g/cm^2$ -thick Formvar side-entrance window are negligible. Baffle- and detector-slit openings were chosen because of low source intensity to give a comparatively large transmission, and the resulting momentum resolution was $\approx 0.25\%$. Spectrometer calibration was determined by measurement of the K -conversion line of the 661.595 ± 0.076 -keV transition⁹ in ^{137}Cs ; the Cs source dimensions were much the same as those of the ^{250}Cf source. Electron momenta were determined by the "upper-edge-intercept" method. Specifically, on a plot, made for each electron line, of count rate vs $\beta\rho$, points on the line's high-momentum side, except for those very near the peak and near the base, fall well on a steep straight line; and the intercept of this straight line with the abscissa at zero count rate may be taken as a measure of electron momentum. When, as was the case here, instrumental resolution is large relative to all natural line widths, use of the intercept method is justified.

There is a recoil problem to be considered in high-resolution measurement of electron lines produced by internal conversion following α decay. An estimate based on the expected transition lifetime and on the stopping power of aluminum for low-kinetic-energy heavy ions¹⁰ shows that in these measurements about 12% of the conversion electrons originated from Cm atoms recoiling in space within a fraction of a mm of the deposited ^{250}Cf activity. The main result of this effect is that in each line there is a 12% component of electrons which had about 0.1% added to their momenta. Appropriate small corrections, made graphically to

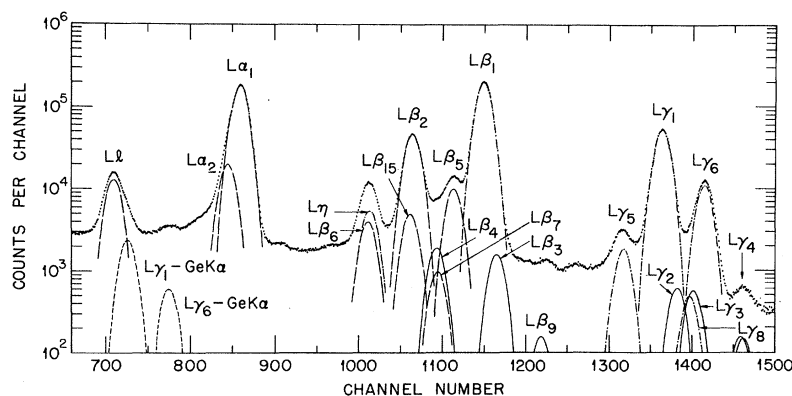


FIG. 1. L x-ray spectrum of curium from the α decay of ^{250}Cf . The dashed-line peaks, the dot-dash-line peaks, and the solid-line peaks in the figure designate x-ray lines resulting from filling of vacancies in the L_3 , L_2 , and L_1 shells, respectively.

each line profile,¹¹ changed the line energies as much as ≈ 10 eV.

TABLE I. Energies and relative intensities of the L x-ray lines and the $2^* \rightarrow 0^*$ γ ray in ^{246}Cm from the decay of ^{250}Cf .

Line designation	Energy (keV)	Relative intensity ($L\beta_1 = 1.000$)	
		Expt.	Theor. ^a
$L\text{I}(L_3 - M_1)$	12.650 ± 0.002^b 12.676 ± 0.020	0.088 ± 0.009	0.078
$L\alpha_2(L_3 - N_4)$	$(14.745 \pm 0.014)^c$		0.121
$L\alpha_1(L_3 - M_2)$	14.959 ± 0.002 14.946 ± 0.020	1.082 0.99 ± 0.03	<u>1.04^d</u>
$L\beta_6(L_3 - N_1)$	$(17.299 \pm 0.016)^e$	$< 0.050 \pm 0.005^e$	0.021
$L\beta_{15}(L_3 - N_4)$	(18.049 ± 0.016)	0.27 ± 0.01	$\left\{ \begin{array}{l} 0.025 \\ 0.228 \end{array} \right.$
$L\beta_2(L_3 - N_5)$	18.113 ± 0.002 18.108 ± 0.020		
$L\beta_7(L_3 - O_1)$...		0.005
$L\beta_5(L_3 - O_{4,5})$...		0.052
$L\eta(L_2 - M_1)$	$(17.331 \pm 0.016)^e$	$< 0.050 \pm 0.005^e$	0.030
$L\beta_1(L_2 - M_4)$	19.426 ± 0.002 19.413 ± 0.018	1.000	<u>1.000</u>
$L\gamma_5(L_2 - N_1)$	21.980 ± 0.008		0.008
$L\gamma_1(L_2 - N_4)$	22.730 ± 0.002 22.717 ± 0.030	0.257 ± 0.006	0.241 0.002
$L\gamma_8(L_2 - O_1)$...		0.002
$L\gamma_6(L_2 - O_4)$	23.519 ± 0.002 23.516 ± 0.020	0.050 ± 0.003	0.049
$L\beta_4(L_1 - M_2)$	(18.568 ± 0.025)		1.00×10^{-2}
$L\beta_3(L_1 - M_3)$	(19.680 ± 0.025)		0.77×10^{-2}
$L\beta_{10}(L_1 - M_4)$	(20.287 ± 0.022)		0.054×10^{-2}
$L\beta_9(L_1 - M_5)$	(20.500 ± 0.024)		0.073×10^{-2}
$L\gamma_2(L_1 - N_2)$	(23.018 ± 0.025)		0.275×10^{-2}
$L\gamma_3(L_1 - N_3)$	(23.318 ± 0.025)		0.244×10^{-2}
$L\gamma'_4(L_1 - O_2)$	(24.219 ± 0.026)	0.133×10^{-2}	<u>0.133×10^{-2}</u>
$L\gamma_4(L_1 - O_3)$	(24.286 ± 0.024)		
γ ray			
$2^* \rightarrow 0^*$ ^{246}Cm	42.852 ± 0.005	0.00583 ± 0.00012 0.0056 ± 0.0005	
$\sum L_1$ lines		0.0255 ± 0.0050^f	
$\sum L_2$ lines		1.35 ± 0.03	
$\sum L_3$ lines		1.60 ± 0.03	

^aTheoretical values are derived from the work of Scofield (Ref. 16) as described in the text.

^bWhere two values are given for the same quantity, the upper member of the pair is that obtained with the photon measuring system of higher resolution.

^cEnergy values in parentheses are calculated from differences between electron binding energies determined in this work (Table III).

^dThe intensities underlined are those of the strongest resolved lines in each L -subshell x-ray group, to which the theoretical intensities of Ref. 16 have been normalized separately in each group.

^eAlthough energies $L\beta_6$ and $L\eta$ are calculated values, a well-resolved peak was observed (Fig. 1) at the energy corresponding to these superimposed lines. The experimental intensity value 0.050 ± 0.005 represents the sum for the two lines.

^fThe intensity sum for L_1 lines is based on the only relatively well-resolved peak of this group, $L\gamma_4$ and $L\gamma'_4$, together with the other group-member intensities as obtained from Ref. 16. Thus the $\sum L_1$ intensity depends heavily on the theoretically known contributions. This is not the case for the $\sum L_2$ and $\sum L_3$ intensities, most of which are derived from well-resolved measured lines.

Photon Spectrometry

Photon spectra from the ^{250}Cf and ^{249}Cf sources were measured in two systems. In the better of these the detector, a Ge(Li) semiconductor 30-mm² area by 5.5-mm depth coupled to a cooled input stage, has a resolution full width at half-maximum (FWHM) of ≈ 250 eV in the Cm L x-ray region and ≈ 480 eV for the K x rays. Radiation entered the detector through a thin Be window. This system, including its 4096 channel analyzer, was carefully calibrated in the range 6–300 keV for small deviations from linearity and for photopeak efficiency with calibrated sources of ^{57}Co , ^{241}Am , ^{113}Sn , ^{203}Hg , ^{137}Cs , ^{243}Am , and ^{240}Pu . Use was made also of an uncalibrated ^{182}Ta source, since the relative intensities and energies of its radiations are very well known.¹² In the other photon measuring system the Ge(Li) detector was larger, 100 mm² by 5 mm; and the resolution was not as high, ≈ 500 eV (FWHM) in the Cm L x-ray region. Energy and efficiency calibrations were based on measurements with standard sources of ^{241}Am (γ 's and Np L x rays) and ^{57}Co .

In order to avoid effects of rate-dependent gain shifts in the energy measurements, γ rays and the Cm L x rays were always recorded simultaneously with reference standards, either U L x rays from ^{240}Pu or Np L x rays from ^{241}Am . For determination of the energy of the $2^* \rightarrow 0^*$ transition in ^{246}Cm , the Eu $K\alpha_2$ and $K\alpha_1$ lines and the $2^* \rightarrow 0^*$ γ ray¹³ emitted following α decay of ^{240}Pu were simultaneously recorded. γ -ray lines from the decay of ^{182}Ta were similarly used as standards for energy measurements of the Cm K series lines emitted in ^{249}Cf decay. These ^{182}Ta lines span the desired region and their energies are known with an accuracy of ≈ 2 eV.¹² Reference K and L x-ray energies were derived from wavelengths given by Bear-den¹⁴ and the recently reevaluated conversion factor

TABLE II. Energies and relative intensities of K x-ray lines in curium ($Z = 96$).

Line designation	Energy (keV)	Intensity ^a
$K\alpha_2(K - L_2)$	104.589 ± 0.005	63.2 ± 0.6
$K\alpha_1(K - L_3)$	109.273 ± 0.005	100
$K\beta_3(K - M_2)$	122.289 ± 0.005	11.2 ± 0.2
$K\beta_1(K - M_3)$	123.407 ± 0.005	23.0 ± 0.5
$K\beta'_2(K - N_{2,3})$	126.982 ± 0.015^b	9.4 ± 0.2
$K_{\text{HO}}(K - O, P)$	128.04	3.5 ± 0.5

^aIntensities are given relative to $K\alpha_1 = 100$. The K -shell fluorescence yield in Cm, ω_K , is greater than 95%.

^bThis value represents the energy at the peak of the observed line. The $K\beta'_2$ line consists, however, of two major components differing in energy by about 300 eV (Table III) and having an intensity ratio about equal to $K\beta_1/K\beta_3$.

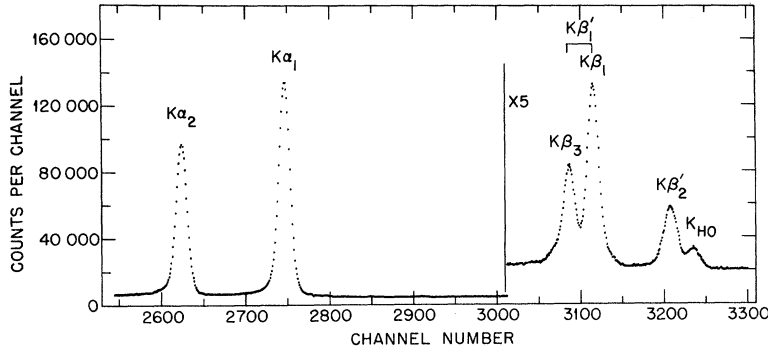


FIG. 2. K x-ray spectrum of curium from the α decay of ^{248}Cf .

of Taylor *et al.*,¹⁵ $E\lambda = 12\,398.301 \pm 0.073 \text{ eV \AA}^*$.

In the system having higher resolution, photopeak centroid positions for the most intense lines could be determined by use of a fitting procedure to ± 0.1 channel, corresponding to energy uncertainty of $\pm 2 \text{ eV}$ for the L x rays or $\pm 5 \text{ eV}$ for the K x rays.

Relative intensities of x-ray lines were determined from photopeak areas by correction for the energy-dependent efficiency, a correction which amounted to approximately 20% between the Cm L1 and the Cm $L\gamma_1$ lines and to about a factor of 2 between the Cm $K\alpha_2$ and $K\beta'_2$ lines. These spectra were obtained separately with sources consisting only of ^{249}Cf or ^{250}Cf .

RESULTS

Photon Energies and Intensities

The Cm L x-ray spectrum observed in ^{250}Cf decay is shown in Fig. 1. Energies and intensities could be determined only for the most intense and well-

resolved lines: L1, $L\alpha_1$, $L\beta_2$, $L\beta_1$, $L\gamma_5$, $L\gamma_1$, and $L\gamma_6$. In order to estimate the intensities of unresolved and weaker lines, the L-shell radiative-transition probabilities calculated by Scofield¹⁶ were extrapolated from $Z=92$ to $Z=96$. These extrapolated probabilities were normalized to the experimental intensity scale separately for each of the three groups of photons arising from vacancy filling in the three L subshells; the $L\alpha_1$, $L\beta_1$, and the two $L\gamma_4$ lines served for normalization of the L_3 , L_2 , and L_1 shells, respectively. Corrections for energy dependence of detector efficiency were included. Energies for most of the unresolved lines could be determined from various combinations of data obtained in this work, and these lines were fitted for comparison with the experimental spectrum, as shown in Fig. 1. The excellent agreement between the fitted curve based on intensity extrapolation and the spectrum observed supports the evaluation, based on the weak $L\gamma_4$ peaks, of the total intensity of L_1 lines. In Table I the experimental values

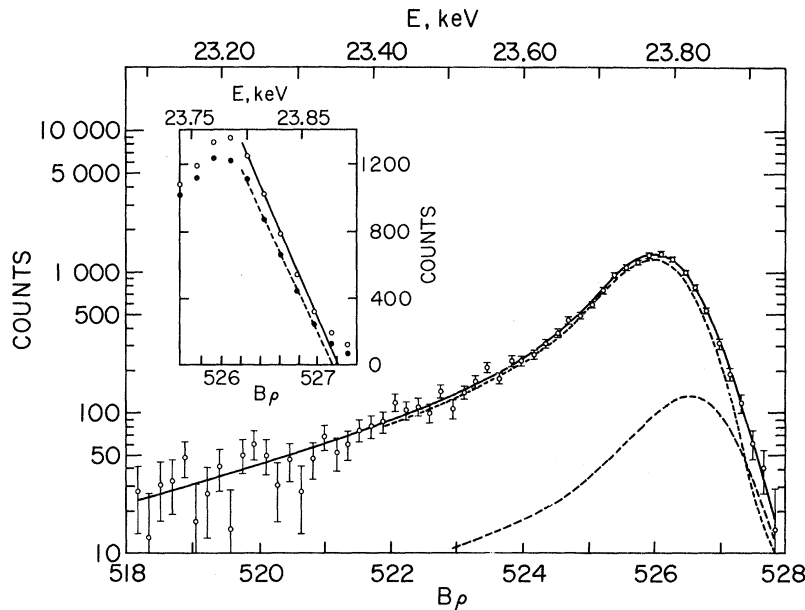


FIG. 3. Electron line produced by internal conversion in the L_3 subshell of the 42.852-keV transition in ^{246}Cm . The upper-edge extrapolation method for electron-momentum determination is shown in the inset along with a correction described in the text. The dashed line is the extrapolation corrected from the measured points on the solid line.

TABLE III. Electron binding energies in curium.

Electron shell	Binding energy (keV)		Scheme for binding energy determination ^c
	Expt. ^a	Theor. ^b	
$K(1s_{1/2})$	128.243 ± 0.006	128.261	$K\alpha_2 + E_B(L_2)$, $K\alpha_1 + E_B(L_3)$, $K\beta_3 + E_B(M_2)$, $K\beta_1 + E_B(M_3)$
$L_1(2s_{1/2})$	24.518 ± 0.021	24.523	$E_\gamma - E_\theta(L_1)$
$L_2(2p_{1/2})$	23.654 ± 0.011	23.654	$E_\gamma - E_\theta(L_2)$
$L_3(2p_{3/2})$	18.973 ± 0.011	18.974	$E_\gamma - E_\theta(L_3)$
$M_1(3s_{1/2})$	6.323 ± 0.011	6.313	$E_B(L_3) - Ll$
	6.297 ± 0.021		
$M_2(3p_{1/2})$	5.946 ± 0.013	5.946	$E_\gamma - E_\theta(M_2)$
	5.954 ± 0.013		$E_B(K) - K\beta_3$
$M_3(3p_{3/2})$	4.839 ± 0.013	4.828	$E_\gamma - E_\theta(M_3)$
	4.836 ± 0.013		$E_B(K) - K\beta_1$
$M_4(3d_{3/2})$	4.228 ± 0.011	4.236	$E_B(L_2) - L\beta_1$
	4.241 ± 0.020		
$M_5(3d_{5/2})$	4.014 ± 0.011	4.014	$E_B(L_3) - L\alpha_1$
	4.027 ± 0.021		
$N_1(4s_{1/2})$	1.674 ± 0.012	1.664	$E_B(L_2) - L\gamma_3$
$N_2(4p_{1/2})$	1.500 ± 0.014	1.493	$E_\gamma - E_\theta(N_2)$
$N_3(4p_{3/2})$	1.200 ± 0.014	1.194	$E_\gamma - E_\theta(N_3)$
$N_4(4d_{3/2})$	0.924 ± 0.011		$E_B(L_2) - L\gamma_1$
	0.937 ± 0.033		
$N_5(4d_{5/2})$	0.860 ± 0.011		$E_B(L_3) - L\beta_2$
	0.865 ± 0.023		
$O_2(5p_{1/2})$	0.299 ± 0.016		$E_\gamma - E_\theta(O_2)$
$O_3(5p_{3/2})$	0.232 ± 0.012		$E_\gamma - E_\theta(O_3)$
$O_4(5d_{3/2})$	0.135 ± 0.011		$E_B(L_2) - L\gamma_6$
	0.138 ± 0.021		
$P_3(6p_{3/2})$	0.033 ± 0.027		$E_\gamma - E_\theta(P_3)$

^aErrors are approximately standard deviations based on uncertainties in the measurements. The result for the K shell is a weighted average. See text for significance of pairs of values.

^bReference 1. Uncertainty in the theoretical values is stated to be ± 0.1% for the K binding energies, ± 0.2% for the L shell and ± 0.5% for the M and N shells.

^c $K\alpha_1$, $L\beta_2$, etc. in this column are photon energies, $E_B(L_3)$ is an electron binding energy, E_γ is the γ -ray energy 42.852 keV, and $E_\theta(M_2)$ is the kinetic energy of the electron from the M_2 subshell internally converted in the deexcitation of the 42.852-keV state of ^{246}Cm .

for energies and intensities of Cm L x rays and unconverted γ rays emitted in ^{250}Cf decay are presented.

In Fig. 2 the Cm K x-ray spectrum from the decay of ^{249}Cf is shown, and the energies and relative intensities are listed in Table II. On the low-energy side of the $K\beta_3$ line there is a small shoulder produced by the $\frac{1}{2}^+ \rightarrow \frac{7}{2}^+$ $E2$ γ transition in the ground-state band¹⁷ of ^{245}Cm . Its intensity relative to that of the $K\alpha_1$ line, about 1.3%, was independent of source-detector distance; and it thus indeed is a crossover transition. Its energy was measured to be 121.711 ± 0.036 keV, in agreement with the reported value 121.5 ± 0.4 keV.¹⁷ The values for the K x-ray energies in Table II agree with the values of Ref. 17 for which no uncertainties are given; there are some minor differences, however, between the Table II intensity values¹⁸ and those of

Hansen *et al.*¹⁹

Electron Binding Energies

One of the more intense electron lines, that originating from internal conversion in the L_3 shell, is shown in Fig. 3. Also illustrated is the linear upper-edge extrapolation method used for electron-momentum determination and the correction for recoil effect. Long counting times were required to obtain the data for the weakest lines.

Electron binding energies in Cm, which were determined, as outlined earlier, from combinations of photon and electron spectrometric data are given in Table III. Accompanying these values is a set of adjusted theoretical values from Ref. 1 and a listing of the data combinations used in arriving at each binding energy. Pairs of values are given for cases in which at least partially independent determination schemes could be used and for cases in which duplicate photon energy values (Table I) were available. The agreement between the theoretical and measured electron binding energies is very satisfying. It should be noted that the values given in Ref. 5 (Table II), which were obtained from interpolation and extrapolation, differ somewhat from the results presented here.

Fluorescence Yields

In addition to the information presented in the tables, values for the fluorescence yields in the L subshells may be obtained from the photon intensity data and the L -subshell internal-conversion coefficients. Recalling that the subshell fluorescence yield ω_i is the probability per vacancy in the i th subshell that a photon is emitted in an electromagnetic transition to that subshell, one obtains the equations

$$\omega_1 = I(\sum L_1) / I_\gamma \alpha_1, \quad (1)$$

$$\omega_2 = I(\sum L_2) / I_\gamma (\alpha_2 + \alpha_1 f_{12}), \quad (2)$$

$$\omega_3 = I(\sum L_3) / I_\gamma [\alpha_3 + \alpha_2 f_{23} + \alpha_1 (f_{13} + f_{12} f_{23})]. \quad (3)$$

In these equations $I(\sum L_i)$ is the intensity sum for all the L x-ray lines corresponding to transitions to the L_i subshell, I_γ is the intensity of the 42.852-keV unconverted γ ray, α_i is the L_i -subshell internal-conversion coefficient of the 42.852-keV transition, and f_{ij} is the Coster-Kronig probability for transfer of the vacancy from the i th to the j th subshell. Internal-conversion-coefficient ratios for this nuclear transition have been measured,⁶ and the results are in accord with theoretical values.²⁰ With the theoretical value 15.7 for α_1 and photon intensities from Table I, Eq. (1) yields directly the result

$$\omega_1 = 0.28 \pm 0.06 .$$

The relatively large uncertainty is associated with the fact that most of $I(\sum L_1)$ has been deduced from its weak $L\gamma_4$ components.

For the evaluation of ω_2 from Eq. (2), knowledge of f_{12} is not critical; α_2 is large in comparison with α_1 and even if f_{12} were as much as $(1 - 0.28) = 0.72$, the contribution of the $\alpha_1 f_{12}$ term would be less than 3%. With $\alpha_2 = 421$ from theory and f_{12} taken to be 0.1, a reasonable choice,²¹ Eq. (2) yields

$$\omega_2 = 0.55 \pm 0.02 .$$

Evaluation of ω_3 from Eq. (3) is fairly straightforward. Here the theoretical value of α_3 , 349,

is comparable with that of α_2 , and f_{23} is therefore important. Recently, McGeorge and Fink have measured this quantity for Cm and have reported $f_{23} = 0.188 \pm 0.019$.²² This result may be compared with a calculated value²³ 0.209 for $Z = 93$ where Coster-Kronig energetics are essentially the same as at Cm. Again, as was the case for evaluation of ω_2 , for ω_3 the α_1 term is unimportant regardless of its f factors. For the sake of completeness the term may be included, and if f_{13} is taken to be 0.55,²¹ one finds

$$\omega_3 = 0.63 \pm 0.02 .$$

Fluorescence-yield data for elements having atomic numbers greater than 94 with which these yields for Cm may be compared are not yet available.

*Research performed under the auspices of the U. S. Atomic Energy Commission.

†Research sponsored by the U. S. Atomic Energy Commission under contract with Union Carbide Corporation.

¹T. A. Carlson, C. W. Nestor, Jr., F. B. Malik, and T. C. Tucker, Nucl. Phys. **A135**, 57 (1969).

²J. M. Hollander, M. D. Holtz, T. Novakov, and R. L. Graham, Arkiv Fysik **28**, 375 (1965).

³I. Ahmad, F. T. Porter, M. S. Freedman, R. F. Barnes, R. K. Sjoblom, F. Wagner, Jr., J. Milsted, and P. R. Fields, Phys. Rev. C **3**, 390 (1971).

⁴P. F. Dittner and C. E. Bemis, Jr. (unpublished).

⁵C. M. Lederer, J. M. Hollander, and I. Perlman, *Table of Isotopes*, 6th ed. (Wiley, New York, 1967).

⁶Y. Y. Chu and M. L. Perlman, Phys. Rev. C **3**, 2021 (1971).

⁷We wish to thank B. Droupesky for arranging the loan of this ²⁵⁰Cf source, which was prepared by C. J. Orth and G. M. Kelley and without which this work could not have been done.

⁸G. T. Emery, W. R. Kane, M. McKeown, M. L. Perlman, and G. Scharff-Goldhaber, Phys. Rev. **129**, 2597 (1963).

⁹J. S. Geiger, R. L. Graham, and F. Brown, Can. J. Phys. **40**, 1258 (1962).

¹⁰L. C. Northcliffe and R. F. Schilling, Nucl. Data Tables, U. S. At. Energy Comm. **7A**, 236 (1970), Fig. 1.

¹¹Such recoil effects on precise energy measurement will be discussed in a forthcoming publication by Y. Y.

Chu and M. L. Perlman.

¹²D. H. White, R. E. Birkett, and T. Thompson, Nucl. Instr. Methods **77**, 261 (1970); R. C. Greenwood, R. G. Helmer, and R. J. Gehrke, *ibid.* **77**, 141 (1970).

¹³M. J. Zender, C. E. Bemis, and M. R. Schmorak, Bull. Am. Phys. Soc. **15**, 1650 (1970).

¹⁴J. A. Bearden, Rev. Mod. Phys. **39**, 78 (1967).

¹⁵B. N. Taylor, W. H. Parker, and D. N. Langenburg, Rev. Mod. Phys. **41**, 375 (1969).

¹⁶J. H. Scofield, Phys. Rev. **179**, 9 (1969).

¹⁷W.-D. Schmidt-Ott, R. W. Fink, and P. Venugopala Rao, Z. Physik **245**, 191 (1971).

¹⁸K x-ray energies and intensities for $Z = 96$ through $Z = 99$ will be the subjects of a future publication by two of the authors (P. F. D. and C. E. B.).

¹⁹J. S. Hansen, H. U. Freund, and R. W. Fink, Bull. Am. Phys. Soc. **15**, 1304 (1970).

²⁰Theoretical values for the L -subshell internal-conversion coefficients were interpolated from the tables of R. S. Hager and E. C. Seltzer, Nucl. Data Tables, U. S. At. Energy Comm. **A4**, 1 (1968).

²¹R. W. Fink, R. C. Jopson, Hans Mark, and C. D. Swift, Rev. Mod. Phys. **38**, 513 (1966). It should be noted that the ordinate on the right of Fig. 9 in this article is incorrect; it should correspond to that in Fig. 10.

²²J. C. McGeorge and R. W. Fink, Bull. Am. Phys. Soc. **16**, 578 (1971).

²³Mau Hsiung Chen, Bernd Crasemann, and Vaclav O. Kostroun, Phys. Rev. A **4**, 1 (1971).